8.6 IMPACT OF TEMPORAL SST VARIATIONS ON A STRATUS-CAPPED MARINE BOUNDARY LAYER

Tracy Haack * and Stephen D. Burk
Naval Research Laboratory, Monterey, CA

1. INTRODUCTION

The U.S. Pacific Coast region exhibits several hallmarks of air-sea processes, such as 1) a pronounced diurnal sea breeze, 2) large SST gradients that may be responsible for altering the character of the observed cloud deck on forecast time scales, and 3) a supercritical marine atmospheric boundary layer (MABL) influenced by synoptic weather modulated by complex orography, persistent coastal upwelling during the spring and summer, and strong diurnal thermal forcing. In this study prior to addressing the fully coupled air-sea problem, emphasis is first placed upon assessing the marine atmospheric boundary layer (MABL) response to SST gradients and temporal variability. This is accomplished by utilizing a series of progressively more realistic process studies simulated by the Coupled Ocean/Atmospheric Mesoscale Prediction System COAMPS™. Specifically we address the structural features of a turbulently forced, cloud-topped MABL that are influenced by temporally varying SST and radiational forcing during a 2 week period in May 1999.

2. MODEL AND PROCESS STUDY DESCRIPTION

In the COAMPS™ version utilized for this study, MABL cloud processes are represented explicitly with the microphysical parameterization of Rutledge and Hobbs (1983). Subgrid scale motions are handled by a 1.5 order closure scheme (Mellor and Yamada 1982). Surface Fluxes of heat, moisture and momentum are given by Louis et al. 1982 with over water roughness governed by the Charnock relation. Radiational forcing is parameterized in the manner described by Harshvardhan et al. (1987). Additional modeling details may be found in Hodur (1997). The 1D model begins the 14 day simulations at 00 UTC (8pm LT) on 16 May 1999.

Initially a 1D COAMPS™ benchmark simulation is established based upon results from a published intercomparison study of LES cloud resolving and 1D models of a stratus-topped MABL (Moeng et al 1996). From that simulation we obtain results for a fixed SST having weak upward surface buoyancy flux. By altering the value of SST we also produce a run with fixed SST and weak downward surface buoyancy flux.

Next we examine the impact upon the MABL cloud structure from realistic SSTs measured at buoy (M1) shown in Figure 1 positioned off of Monterey Bay, CA. During a two week period in May of 1999 the buoy recorded a ~3°C increase in SST with the

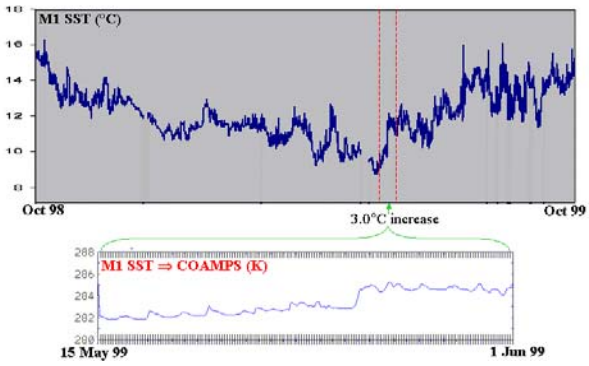

Figure 1: M1 buoy measurements of SST (°C) for Oct 98 - Oct 99, and COAMPS™ SST (K) 15 May – 1 Jun 99.

*Corresponding author:
Tracy Haack, Naval Research Laboratory, 7 Grace Hopper Ave., Monterey, CA 93943-5502; haack@nrlmry.navy.mil

bulk of the change occurring over 10 hours. Owing to the initial choice of temperature profile, which matched that of the Moeng study, this simulation was controlled by weakly stable surface stability. Subsequently, two additional sensitivity tests are performed using the same observed M1 SSTs but by adding a constant increment to obtain a case with 1) stable to unstable surface flux transition and 2) completely unstable surface fluxes.

Finally, from a 3D idealized COAMPS™ simulation using the fixed SST and homogeneous initial condition specified by Moeng, we study the 3D response of a coastal stratus deck to complex coastal topography, diurnal forcing, and weak upward surface buoyancy flux. The single mesh domain is situated over coastal CA and OR, has 9 km horizontal resolution, and 60 vertical levels with more than 25 in the lowest 1 km at 50 m or better vertical spacing.

2. FIXED SST 1D SIMULATIONS

Using a fixed SST value at 288 K and the Moeng et al (1996) initial conditions with light winds (~4.5 ms^{-1}), COAMPS^{TM} results at hour 2 are compared to the published LES profiles. Generally good agreement is found in the magnitude, height and depth of max/min of various turbulent, MABL and cloud parameters. In COAMPS^{TM} however, the TKE peak is at or near the base of the cloud, ~125m lower than the LESs, and does not produce a secondary maximum at the surface owing to the assumption of isotropic turbulence as a lower boundary condition. Hence, the cloud top height in COAMPS^{TM} is slightly lower (by ~50 m), while the peak value and depth are consistent with the LESs.

In the 2-week simulations radiation permits longwave cooling and diurnally varying shortwave warming to influence the MABL environment. Cloud top cooling within the MABL produce a case with unstable upward surface sensible heat, latent heat, and buoyancy fluxes. The interaction of the radiative forcing with the cloud moisture produces diurnal perturbations in near surface temperature, wind speed, water vapor and fluxes, which drive diurnal variations in integrated, cloud liquid water content (ICLW). As shown in Figure 2, ICLW perturbations peak near the middle of the two weeks oscillating between 0.5 and 2.0 kg m^{-2} (lower line in Fig. 2). For comparison, a stable case with negative surface fluxes is also presented having fixed SST = 283 K. Note that with stable fluxes a much more steady behavior is obtained in the time series (upper line). And, these ICLW values have 3 times the average magnitude of the unstable regime and contain a larger diurnal amplitude.

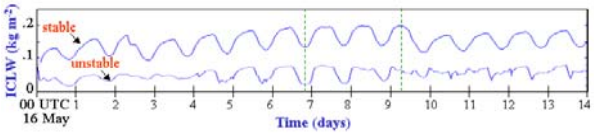

Figure 2: Time series of ICLW (kg m^{-2}) beginning 00 UTC (8pm LT) 16 May 1999 for the stable and unstable fixed SST cases.

Profiles of cloud liquid water mixing ratio (q_c), at times corresponding to the max/min values of ICLW for 64 hours near the middle of the 2 weeks are shown in Figure 3.

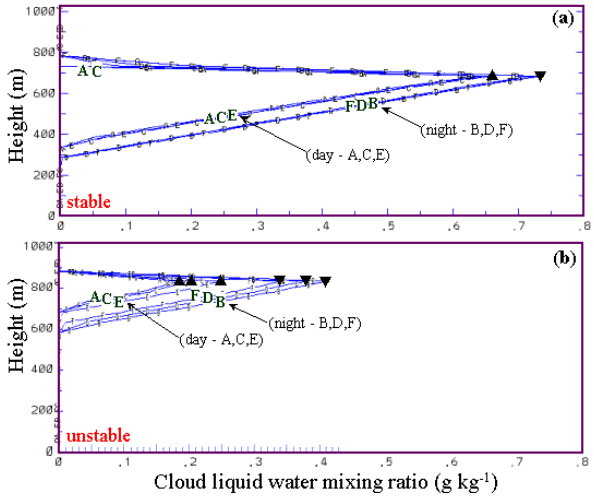

Figure 3: Profiles of q_c (g kg^{-1}) for fixed SST at 8am LT (night) and 4pm LT (day) over a 64 hour period (dashed lines in Fig. 2) for the stable (a), and unstable (b) cases. The up triangle indicates the daytime minimum and the down triangle the nighttime maximum in q_c.

The maximum q_c tends to occur near sunrise at ~8am LT, and the minimum near peak heating at ~4pm LT. In this figure, diurnal trends in the cloud layer are compared as well as the effect of stable and unstable surface forcing for fixed SST. This figure reveals a cloud layer that is 40-50% thicker and moister in the stable case. Layer thinning occurs at both cloud top and bottom during the day as the MABL warms. Profiles for the unstable case show the lifting of cloud base only, and consistent with the ICLW time series, yield larger diurnal amplitudes in q_c than in the stable case.

3. TEMPORALLY VARYING SST 1D SIMULATIONS

In this section results from utilizing the M1 buoy measurements, with differing surface stabilities, are described. Because the unaltered M1 SSTs are several degrees cooler than the initial MABL temperature in the Moeng study, this first M1 simulation is a stable one with weak downward surface fluxes. The initial state is consistent with the stable fixed SST case presented in Section 2. Latent heat fluxes are slightly negative initially until after the rapid ~3° increase in SST which occurs on day 7 at ~8am LT. Immediately following the SST jump, surface buoyancy, latent and sensible heat fluxes increase and become much more unsteady. As shown in the ICLW time series of Figure 4, the cloud layer's response to the SST jump in this stable case is a rapid damping of the diurnal signal and substantial reduction in ICLW (Fig. 4, upper line). This response is due primarily to the change in sign of the latent heat flux as the surface saturation specific humidity becomes greater than that at 10 m.

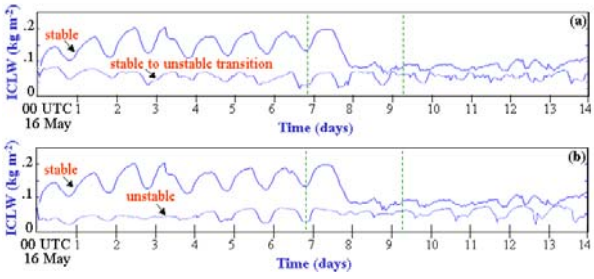

Figure 4: Time series of ICLW (kg m^{-2}) for the M1 temporally varying SST (a) stable and transitional cases and (b) stable and unstable case.

Examination of the vertical profiles over the 64-hour period encompassing the SST jump yields a dramatically different MABL response in comparison to the stable fixed SST case (Fig. 3a). After the jump, turbulence within the cloud layer increases and peak TKE values at nighttime are almost twice as large as the fixed simulation. Figure 5a shows the profiles of q_c for this case. With the additional TKE mixing, cloud liquid water diminishes after the jump, especially at night where maximum values have dropped by ~40% of those for fixed SST. Additionally, the consistent but subtle diurnal modulation of the cloud layer in the fixed SST case is not seen in this simulation. After the SST jump during both day and night, the layer thins 50-150 m and elevates 100-200 m.

For simulations with varying SST, we

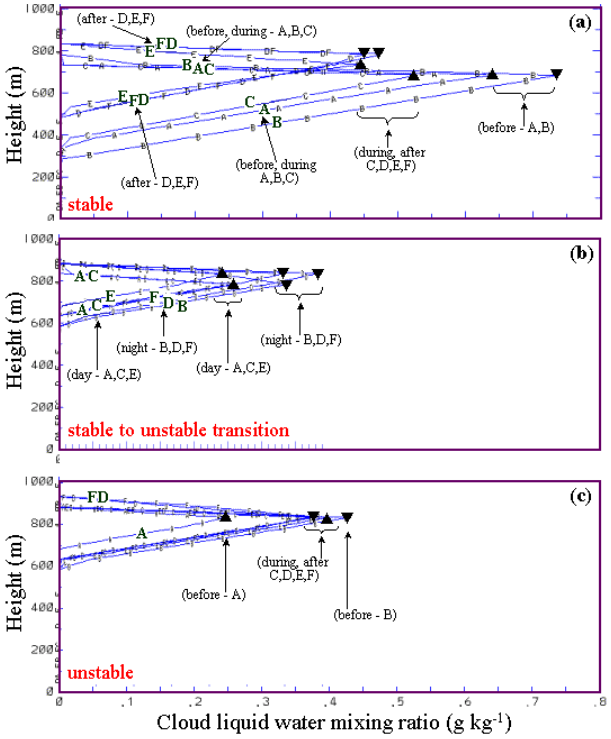

Figure 5: As in Fig. 3 except for the M1 temporally varying SST stable (a), transitional (b) and unstable (c) cases. Diurnal trends and pre/post SST jump trends are denoted by the arrows.

also produce two sensitivity tests: a stable to unstable transition case and a purely unstable case by adding a constant increment to the M1 buoy measurements. For the unstable case, the time series of ICLW (Fig. 4b, lower line) is not very different than for a fixed SST (Fig. 2, lower line) although the weak diurnal oscillations are suppressed during and after the rapid SST increase at day ~7.5. The ICLW then recovers to a larger diurnal amplitude as the MABL reaches a new equilibrium with moister cloud liquid water than in the fixed SST case.

In Figure 5b,c, the day/night q_c profiles for the two sensitivity tests are shown. We first examine the purely unstable case (Fig. 5c). In comparing to the unstable fixed SST results (Fig. 3b), several effects are noted with respect to the cloud layer *after the SST jump*: 1) During the day the cloud base height and peak values of q_c remain similar to the nighttime profiles rather than going through the diurnal oscillation seen in Fig. 3b for the unstable fixed SST case. 2) The cloud top height contains diurnal variation not present in the fixed SST case. During the night a combination of higher daytime q_c values, greater cloud top cooling, and increased turbulence lifts the cloud top ~50 m higher than with a fixed SST.

For the transitional stability case of Fig. 5b, the q_c profiles maintain the diurnal trends present in the fixed SST cases (Fig. 3) albeit with weaker peak q_c values. As in the temporally varying stable SST case, both cloud base and top elevate in response to the increased SST.

4. 3D IDEALIZED STRATUS SIMULATIONS

In this 3D simulation, situated over the U.S. west coast, the additional complexity of detailed coastal topography on the diurnal behavior of the cloud deck is currently being studied. Utilizing a homogeneous field of idealized initial conditions from Moeng et al (1996) with fixed SST, the diurnal changes in the offshore cloud field are similar to those of the 1D fixed unstable SST case presented in Sec. 2. Figure 6 shows comparable night/day magnitudes in ICLW revealing the reduction in daytime ICLW as shortwave radiation warms the MABL slightly and lifts cloud base. Closer to the coast, 3D mesoscale detail is apparent in the cloud field as the MABL is modulated by the intricacies of the coastal orography interacting with the synoptic flow and local sea/land breeze forcing. Enhanced nighttime cloudi-

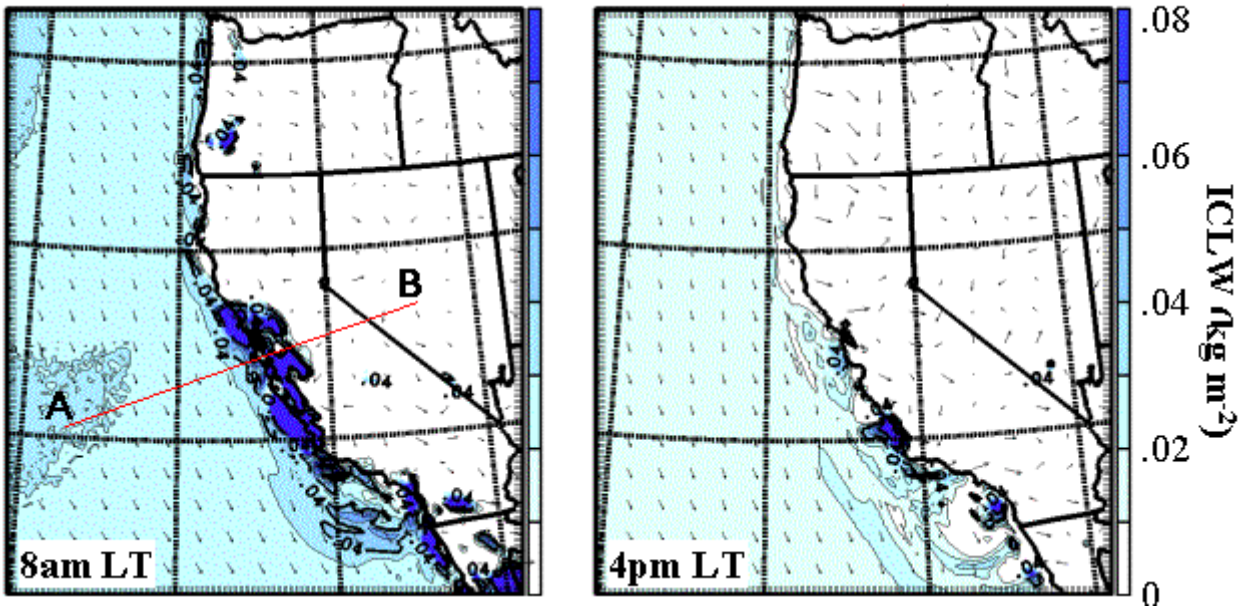

Figure 6: Horizontal distribution of ICLW (kg m^{-2}) at 8am and 4pm LT for the 3D unstable fixed SST case.

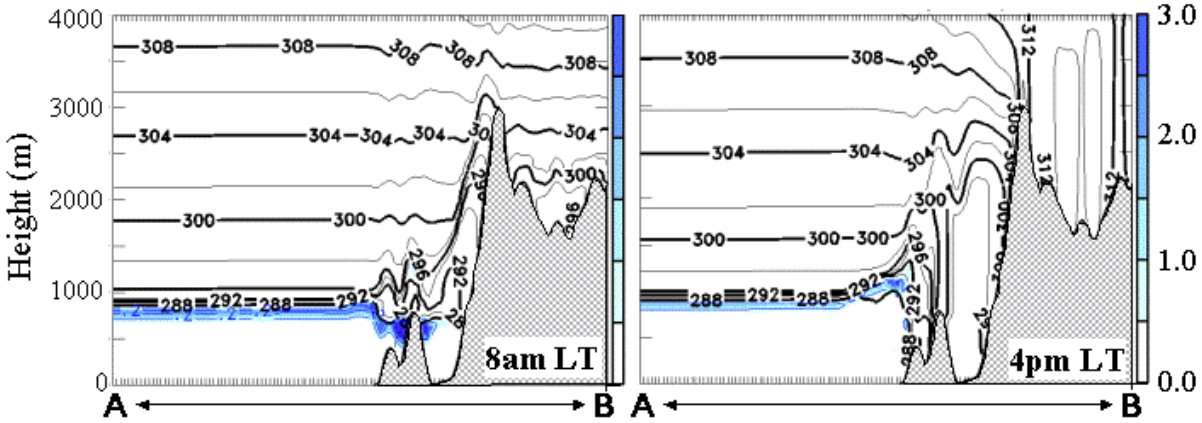

Figure 7: Vertical cross-section of q_c (g kg^{-1}) shaded, and potential temperature (K) isolines at 8am and 4pm LT along line A-B of Fig. 6.

ness forms along the central coast encroaching inland and down valleys. With daytime heating clearing has occurred in regions along the coast while heavy stratus tends to persist north of Pt. Conception throughout the afternoon.

To obtain a vertical view of the MABL structure and cloud characteristics, Figure 7 displays cross-sections along line A-B of Fig. 6 showing q_c (shaded) and potential temperature (isolines) for the same day/night times as in Fig. 6. Offshore cloud features are in general agreement with the 1D unstable fixed profiles (Fig. 3b). Near the coast however, we note the evolution of the stratus deck with diurnal forcing. The cloud layer has lowered and moistened by 8am LT over the coastal mountain range and within ~50 km of shore, while by afternoon it has cleared over land becoming thinner, patchy, and elevated over water within ~100 km of shore.

The 3D results are preliminary and require additional study of the turbulence and radiational terms driving the local mesoscale variations in the cloud field. In the future we also anticipate sensitivity tests with differing surface stability using this more realistic 3D domain with complex coastal topography.

Acknowledgments. We are grateful to Drs. Julie Pullen and John Kindle for their contributions to the research. This work is supported by The Office of Naval Research, Program Element 0601153N.

REFERENCES

Louis, J.F., et al 1982: A short history of the operational PBL parameterization at ECMWF, *Workshop on Planetary Boundary Parameterization,* ECMWF, Reading, 59-79.

Mellor, G.L. and T. Yamada, 1982: Development of a turbulence closure for geophysical fluid problems. *Rev. Geophys and Space Phys.*, **20**, 851-875.

Moeng, C.-H., et al. 1996: Simulation of a stratocumulus topped planetary boundary layer: Intercomparison amount different numerical codes. *Bull. Amer. Meteor. Soc.*, **77**, 261-278.

Harshvardhan, R.D., D. Randall, and T. Corsetti, 1987: A fast radiation parameterization for atmospheric circulation models. *J. Geophys.Res.*, **92**, 1009-1016.

Hodur, R.M., 1997: The Naval Research Laboratory's coupled Ocean/ atmosphere mesoscale prediction system (COAMPS). *Mon. Wea. Rev.,* **125**, 1414-1430.

Rutledge, S.A., and P.V. Hobbs, 1983: The mesoscale and microscale structure of organization of clouds and precipitation in midlatitude cyclones. VIII: A model for the "seeder-feeder" process in warm-frontal rainbands. *J. Atmos. Sci.,* **40**, 1185-1206.